

# Detection of strong activity in the eclipsing binary brown dwarf 2MASS J05352184–0546085 – A possible explanation for the temperature reversal

A. Reiners\*, A. Seifahrt

*Institut für Astrophysik, Georg-August-Universität, Friedrich-Hund-Platz 1, D-37077  
Göttingen*

[Ansgar.Reiners, seifahrt]@phys.uni-goettingen.de

K.G. Stassun

*Department of Physics and Astronomy, Vanderbilt University, Nashville, TN 37235*

keivan.stassun@vanderbilt.edu

C. Melo

*European Southern Observatory, Casilla 19001, Santiago 19, Chile*

cmelo@eso.org

and

R.D. Mathieu

*Department of Astronomy, University of Wisconsin – Madison, Madison, WI 53706*

mathieu@astro.wisc.edu>

## ABSTRACT

We show high resolution spectra of the eclipsing brown dwarf binary 2MASS J05352184–0546085 taken at the two opposite radial velocity maxima. Comparisons of the TiO bands to model and template spectra are fully consistent with the temperatures previously derived for this system. In particular, the reversal of temperatures with mass – in which the higher-mass primary is cooler than its companion – is confirmed. We measure the projected rotation velocities

---

\*Emmy Noether Fellow

of the components; the primary is rotating at least twice as rapidly as the secondary. At the two radial velocity maxima, H $\alpha$  emission lines of both components stick out to either sides of the H $\alpha$  central wavelength, which is dominated by nebula emission. This enables us to model the individual H $\alpha$  lines of the primary and the secondary. We find that the H $\alpha$  emission from the primary is at least 7 times stronger than the emission from the secondary. We conclude that the temperature reversal is very likely due to strong magnetic fields inhibiting convection on the primary.

*Subject headings:* binaries: eclipsing – stars: low-mass, brown dwarfs – stars: magnetic fields – stars: individual (2MASS J05352184-0546085)

## 1. Introduction

2MASS J05352184–0546085 (hereafter 2MASS 0535–0546) is the first known eclipsing binary system comprising two brown dwarfs (Stassun et al. 2006), with dynamically measured masses of  $M_1 = 56 \pm 4 M_{\text{Jup}}$  and  $M_2 = 36 \pm 3 M_{\text{Jup}}$ . The large component radii of  $R_1 = 0.67 \pm 0.03 R_{\odot}$  and  $R_2 = 0.49 \pm 0.02 R_{\odot}$  suggest that the brown dwarfs are very young, and indeed the system satisfies kinematic and distance criteria for membership in the Orion Nebula Cluster (M42, age  $\sim 1$  Myr). Providing the only direct and precise measurements to date of the fundamental physical properties of young brown dwarfs, 2MASS 0535–0546 represents an important opportunity to test and calibrate theoretical models of brown dwarf formation and early evolution.

Remarkably, 2MASS 0535–0546 exhibits a reversal of effective temperatures: The lower-mass secondary is warmer than the higher-mass primary. The ratio of effective temperatures,  $T_2/T_1$ , is  $1.064 \pm 0.004$  (Stassun et al. 2007, hereafter SMV07). Such a temperature reversal is not predicted by any current models of brown dwarf evolution.

One possible explanation for this temperature reversal considered by SMV07 is that convection in the primary has been somehow suppressed, perhaps through the presence of a strong surface field on the primary brown dwarf. In this Letter we present high-resolution spectra of 2MASS 0535–0546 which (a) provide independent confirmation of the temperature reversal, and (b) reveal that the primary is indeed much more magnetically active than the secondary.

## 2. Data

Data were obtained with the UVES spectrograph at ESO/VLT in March and April, 2006 (proposal ID 276.C-5054). Two exposures of 2MASS 0535–0546 were taken close to the two radial velocity maxima. We give in Table 1 the date of observation, orbital phase, radial velocities, and seeing conditions at the end of each exposure. The radial velocity curve for the orbital solution of 2MASS 0535–0546 can be found in SMV07. We did not compute a new orbital solution because the one given in SMV07 is already well constrained and the orbit is well covered. Hence we do not expect significant improvements from the new data.

Observations were taken with the slit opened to  $1.1''$  ( $R \approx 36,000$ ) and the CCD was used in  $2 \times 2$  binning mode. Exposure times were 3600 s. UVES was used in dichroic mode with the blue arm centered at 437 nm and the red arm centered at 760 nm providing wavelength coverage from 3730 Å to 9460 Å with only a few gaps. Because of the target’s faintness and red color, however, a low signal-to-noise ratio (SNR) is reached below 7000 Å. Redward of 7000 Å, the SNR is around 10 per pixel.

Data were corrected for cosmic rays, bias- and dark-subtracted and flatfielded in standard fashion using echelle reduction routines based on the MIDAS UVES pipeline package. Sky emission was removed by subtracting the mean of two sky spectra extracted above and below the target spectrum in direction perpendicular to dispersion. After 3600 s of exposure the night sky provides a significant contribution to the spectrum in the form of sky emission lines. These lines are mainly due to OH (Osterbrock et al. 1996; Hanuschik 2003) and can generally be removed easily. Furthermore, 2MASS 0535–0546 sits in the Orion nebula that imprints a rich spectrum of strong emission lines (Esteban et al. 2004). The spectral regions of the strongest nebula emission lines are entirely dominated by nebula lines, so that the much weaker contribution of the target spectrum cannot be restored in the centre of the nebula emission lines. This is particularly problematic at the two hydrogen lines contained in the spectra,  $H\alpha$  and  $H\beta$ .

## 3. Temperatures

SMV07 found that the two components of 2MASS 0535–0546 have very similar spectral types of  $\sim M6.5 \pm 0.5$ , implying  $T_{\text{eff}} \approx 2700$  K. The ratio of the two components is fixed from the ratio of the eclipses,  $T_2/T_1 = 1.064 \pm 0.004$ . Absolute temperatures could only be derived from spectral types implying uncertainties on the order of  $\sim 200$  K.

The two TiO bands at 7050 Å ( $\gamma$ -band) and 8430 Å ( $\epsilon$ -band) are particularly temperature sensitive (but gravity insensitive). At the times of radial velocity maxima, both bandheads

can be disentangled allowing us to model the spectra of both components. We tried to determine individual temperatures by comparing the data at highest radial velocity difference (spectrum #2 in Table 1) to the sum of two reference spectra. For the reference spectra we tried both synthetic model spectra and empirical template spectra (see below). In both cases we assume the radial velocity difference from the orbital solution of SMV07.

First, we try to determine the temperatures from PHOENIX models of the DUSTY series (see Allard et al. 2001). Reiners (2005) has shown that the  $\gamma$ - and the  $\epsilon$ -bands yield significantly different results in early M stars, a discrepancy probably due to uncertain oscillator strengths mainly in the  $\epsilon$ -band. While temperatures derived from the  $\gamma$ -band are consistent with temperatures in M1–M5.5 stars with interferometrically measured radii, results for the  $\epsilon$ -band temperatures are too low. Hence we use the synthetic spectra only in the  $\gamma$ -band. The synthetic spectra are consistent with the temperature ratio derived by SMV07. The best fit is achieved with  $T_{\text{eff},1} = 2850$  K and  $T_{\text{eff},2} = 3000$  K. On the other hand, these absolute temperatures are a little high compared to the results from the  $JHK$  magnitudes (SMV07). This is probably due to a temperature overestimate of the model spectra; in this temperature regime, the model TiO  $\gamma$ -bands differ from observed spectra in the sense that observed TiO bands show a reversal of depth with temperature around 2700 K. This dust-induced effect is not fully captured by the models we used (Mohanty et al. 2004); in the model spectra the  $\gamma$  bands just keep saturating. The  $\gamma$ -band has lost its high diagnostic capabilities at such low temperatures. Thus, while our best fit yields temperatures consistent with the temperature reversal found by SMV07, in truth such a small temperature difference as in the two components of 2MASS 0535–0546 cannot be robustly tested in our spectra of the  $\gamma$ -band.

In the TiO  $\epsilon$ -band, to circumvent known problems with the PHOENIX models (Reiners 2005), we compare our data to template spectra of single M stars observed during the same campaign. Template stars observed are LHS 292 (M6.5,  $\sim 2750$  K) and GJ 3877 (LHS 3003, M7,  $\sim 2650$  K). Temperatures are from Golimowski et al. (2004). We note that these temperatures assume a certain radius and very high age for the template stars. The temperatures could be lower by about 300 K if the template stars were young. We took the luminosity ratio and radial velocities from the orbital solution as above. We show the  $\epsilon$ -band of 2MASS 0535–0546 in Fig. 1 (black). The red line shows our best fit, a sum of the weighted spectra of LHS 292 for the hotter component and of GJ 3877 for the cooler component. This combination yields a very good match to the spectrum of 2MASS 0535–0546. Hence our data is consistent with temperatures 2650 K and 2750 K for the two components in good agreement with  $JHK$  temperatures. We can also test the hypothesis that the primary is hotter than the secondary, which is a possible alternative from the fit to radial velocities and the photometric light curve if the radii are reversed instead of the temperatures (SMV07).

We show the result as a grey line in Fig. 1. Clearly, this alternative yields strong deviations from the data around 8435 Å and 8443 Å. Formally, the fit qualities of the red and the grey models in Fig. 1 are different by  $\Delta\chi^2 = \chi_{\text{red}}^2 - \chi_{\text{grey}}^2 = 5.5$  (for a SNR of 10 and a reduced  $\chi_{\nu}^2 = 1.16$ ). This means that the difference is significant on a  $2\sigma$ -level.

#### 4. Rotation and Activity

We measure the projected rotation velocities  $v \sin i$  via cross correlation with the spectrum of GJ 1057 (M5) observed during the same campaign (cp. Reiners & Basri 2006). Several orders are used and we consistently find the primary to be more rapidly rotating than the secondary. We estimate our uncertainties to be  $5 \text{ km s}^{-1}$  due to low SNR and the fact that two objects are in the spectra. Our results are given in Table 2; we find  $v \sin i = 10 \text{ km s}^{-1}$  for the primary and do not detect significant rotation in the secondary, i.e.  $v \sin i < 5 \text{ km s}^{-1}$ .

Indicators of magnetic activity are emission in the CaII H & K lines (3934 Å and 3968 Å), or in the Ca triplet lines at 8498 Å, 8542 Å, and 8662 Å. All five Ca lines are covered by our spectra, but typical Ca emission in active M dwarfs is relatively low (unless observed during a flare). In our spectra, we do not detect significant emission in any of the Ca lines. The strongest indicator of magnetic activity in M-type stars is emission in H $\alpha$ . This line, however, is also emitted in HII regions like the Orion nebula in which 2MASS 0535–0546 is located. Flatfielded and cosmic-ray corrected echellograms at the region of H $\alpha$  are shown in Fig. 2. The spectrum of 2MASS 0535–0546 appears horizontally at pixel 490 on the Y-axis. Around the region of H $\alpha$ , we identified three emission lines that do not come from 2MASS 0535–0546. They are spatially extended and can be subtracted using the area of the slit adjacent to the target spectrum. The components are: a) the strong H $\alpha$  nebula line, b) the weak deuterium nebula line (Hébrard et al. 2000), and c) the night sky emission line of H $\alpha$ . In these features, we see no variation between the two exposures. Because 2MASS 0535–0546 is comoving with M42, the two brown dwarfs produce spectral lines fluctuating around the spectral lines of M42. Hence the central part of 2MASS 0535–0546’s H $\alpha$  emission is obscured by the massive nebula lines, but during the two radial velocity maxima the H $\alpha$  lines of the two components move close to the outer edge of the nebula emission line, and they clearly appear in the raw image in Fig. 2.

In Fig. 3, we show the two spectra of 2MASS 0535–0546 after subtracting the nebular and the night sky emission lines. The black line shows spectrum #1 and the red line shows spectrum #2 of Table 1. In the inset, we show the reduced spectra without subtraction of the background emission. Note that the units are the same as in the inset, i.e. that the nebula line emission peak is roughly a factor 50 stronger than the object’s emission that we

detect in the residuals. Hence the absolute photon noise of the nebula line emission is on the order of 200 and renders a proper analysis in the central region of the nebula emission impossible.

It is clear from Figs. 2 and 3 that strong  $H\alpha$  emission is emitted by 2MASS 0535–0546, and that its main component is shifted to the red in spectrum #1 (black line) and to the blue in spectrum #2 (red line). The data show that the primary emits very strong  $H\alpha$  emission. To quantify  $H\alpha$  emission in both components, we attempted a two component fit to the data. We assume a Gaussian shape of the  $H\alpha$  emission profiles for both components, which is justified because we see no evidence for accretion. We keep the positions of the two Gaussians fixed at the wavelengths according to their radial velocities. We assume that in both exposures the strength of each emission component is constant, i.e. the individual equivalent widths do not vary between the two exposures. The only free parameters in our fit are the amplitude and the width of the Gaussians. However, because we do not see the maxima of the emission lines, amplitude and width particularly of the primary component's emission are degenerate.

A fit to the data is overplotted in Fig. 3, dotted lines show the individual emission from the two components. Black and red color corresponds to spectra #1 and #2, respectively (same color as the data). In spectrum #1, we see only the redshifted emission flank from the primary. No significant emission is found on the blue side of the gap. In the second spectrum, however, we see the blueshifted emission from the primary and a small emission component on the red side.

Our fit shows the solution with the lowest possible emission contrast between the two components, i.e. smallest emission from the primary and largest emission from the secondary. For this case, we measure individual  $H\alpha$  equivalent widths of  $32.6 \text{ \AA}$  for the primary and  $4.8 \text{ \AA}$  for the secondary. One could easily fit the primary emission using a higher amplitude for the Gaussian emission at smaller width implying stronger primary emission. On the other hand, the secondary emission is relatively well constrained from spectrum #2, and from spectrum #1 it looks like our result is even a little on the high end. Thus, our measurements of  $H\alpha$  equivalent widths should be interpreted as a lower limit for the primary of 2MASS 0535–0546, and as an upper limit for the secondary. The  $H\alpha$  equivalent width of the primary is at least a factor 7 larger than the emission from the secondary.

## 5. Conclusions

We have used high resolution spectra of 2MASS 0535–0546 taken at radial velocity maxima to investigate the temperature reversal of this enigmatic brown dwarf binary. We used two TiO bands to constrain the absolute temperatures of the two components. In the  $\gamma$ -band, we have used PHOENIX model spectra, but it is not clear to what extent these models can accurately reproduce the real TiO spectra. From the model spectra, we find temperatures of 2850 K and 3000 K ( $\pm 120$  K) for the primary and secondary, respectively. In the  $\epsilon$ -band, we have used spectra from stellar templates yielding much lower temperatures, but effects of metallicity may introduce differences between template spectra and the spectrum of 2MASS 0535–0546. This method yields temperatures between 2600 K and 2750 K. Most importantly, the  $\epsilon$ -band analysis confirms the finding by SMV07 of a temperature reversal in this system, such that the higher-mass primary is indeed cooler than the lower-mass secondary.

A possible explanation for the temperature reversal may be that large scale magnetic fields are inhibiting convection. In low mass stars, magnetic fields manifest themselves for example as  $H\alpha$  emission, and at least in sun-like stars activity is correlated to the rotation rate. We find that the primary of 2MASS 0535–0546 shows at least 7 times stronger activity than the secondary, and the former is also rotating at least a factor of 2 more rapidly than the latter.

We can convert the equivalent widths into normalized  $H\alpha$  luminosities (see Reiners & Basri 2007). We find  $\log L_{H\alpha}/L_{\text{bol}} = -3.47$  and  $-4.30$  for the primary and secondary components, respectively. Reiners & Basri (2007) have measured  $H\alpha$  luminosities and magnetic fields in a sample of M dwarfs. They found that for a given spectral type  $H\alpha$  is closely correlated with magnetic field. From the normalized  $H\alpha$  luminosities of 2MASS 0535–0546 we can estimate the mean magnetic flux on its two components. The primary’s  $H\alpha$  luminosity of  $\log L_{H\alpha}/L_{\text{bol}} = -3.47$  is on the top end of  $H\alpha$  luminosities found among M6–M7 dwarfs and indicate a very high magnetic flux level of  $Bf \approx 4$  kG over the entire object (cp. left panel of Fig. 12 in Reiners & Basri 2007). The secondary’s  $H\alpha$  luminosity is only around average for that spectral range (see also West et al. 2004) and indicates significantly weaker magnetic flux of  $Bf \approx 2$  kG.

Recently, Chabrier et al. (2007) have shown that the effect of inhibited convection could indeed explain the temperature reversal in 2MASS 0535–0546. They suggest that magnetic fields with surface values of a few kG might be sufficient for severely inhibiting convection in parts of low mass star interiors. The observations presented here support this scenario.

We thank Michael Sterzik, it was his idea to obtain such a data set. Based on observations collected at the European Southern Observatory, Paranal, Chile, 276.C-5054. A.R. has received research funding from the DFG as an Emmy Noether fellow (RE 1664/4-1). A.S. acknowledges funding from the DFG (RE 1664/4-1). K.G.S. gratefully acknowledges support from National Science Foundation Career grant AST-0349075 and from a Research Corporation Cottrell Scholar award. R.D.M. acknowledges NSF Grant AST-0406615.

## REFERENCES

- Allard, F., Hauschildt, P.H., Alexander, D.R., Tamanai, A., & Schweitzer, A., 2001, *ApJ*, 556, 357
- Chabrier, G., Gallardo, J., & Baraffe, I., 2007, *A&A*, 472, L17
- Esteban, C., Peimbert, M., García-Rojas, J., Ruiz, M.T., Peimbert, A., & Rodríguez, M., 2004, *MNRAS*, 355, 229
- Hébrard, G., Péquino, D., Walsh, J.R., Vidal-Madjar, A., & Ferlet, R., 2000, *A&A*, 364, L31
- Hanuschik, R.W., 2003, *A&A*, 407, 1157
- Golimowski, D.A., Leggett, S.K., Marley, M.S., et al., 2004, *AJ*, 127, 3516
- Mohanty, S., Basri, G., Jayawardhana, R., Allard, F., Hauschildt, P.H., & Ardila, D., 2004, *ApJ*, 609, 854
- Osterbrock, D.E., Fulbright, J.P., Martel, A.R., Keane, M.J., Trager, S.C., & Basri, G., 1996, *PASP*, 108, 277
- Reiners, A., 2005, *AN*, 326, 10, 930
- Reiners, A., & Basri, G., 2006, *AJ*, 131, 1806
- Reiners, A., & Basri, G., 2007, *ApJ*, 656, 1121
- Stassun, K.G., Mathieu, R.D., & Valenti, J.A., 2007, *ApJ*, 664, 1154 (SMV07)
- Stassun, K.G., Mathieu, R.D., & Valenti, J.A. 2006, *Nature*, 440, 311
- West, A.A., Hawley, S.L., Walkowicz, L.M., et al., 2004, *ApJ*, 128, 426

Table 1. UVES observations of 2M0535–05.

#	JD <sup>a</sup> - 2 453 800	Orbital phase	Seeing	$v_{\text{rad}}[\text{km s}^{-1}]$	
				prim	sec
1	31.49344	0.2445–0.2487	1.40''	+12.6	–20.0
2	28.49346	0.9377–0.9420	1.25''	–23.2	+36.7

<sup>a</sup>Julian Date at start of observation

Table 2. Rotation and activity of 2MASS 0535–0546.

	$v \sin i$ [km s <sup>-1</sup> ]	$\log L_{\text{H}\alpha}/L_{\text{bol}}$
Primary	10	-3.47
Secondary	< 5	-4.30

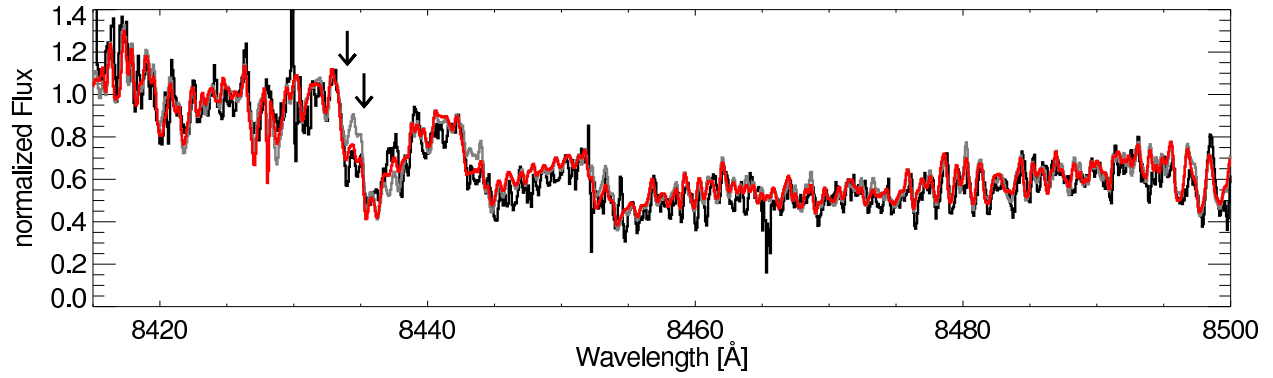


Fig. 1.— Absorption band of TiO ( $\epsilon$ -band). Data are shown in black. The two fits are the sum of two observed template spectra. The red line is calculated with a lower temperature for the primary component, the grey line shows the spectrum for reversed temperatures (see text).

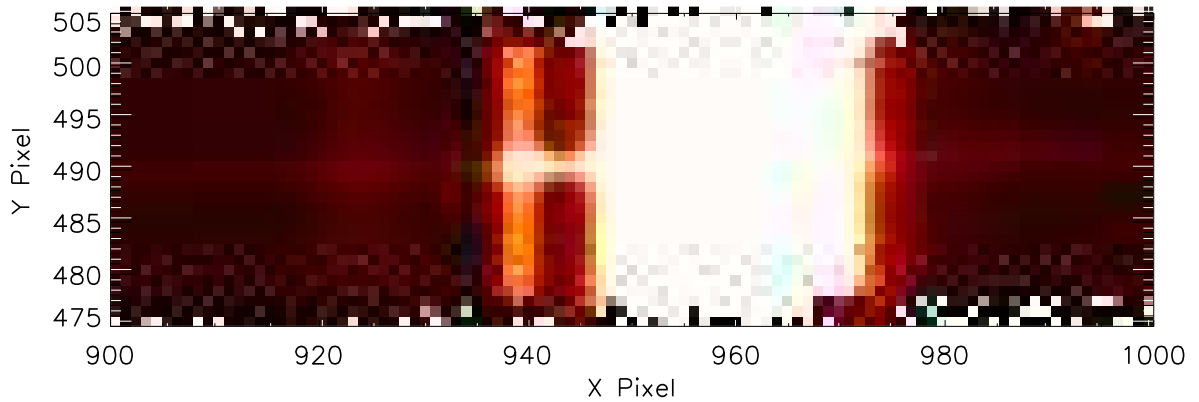
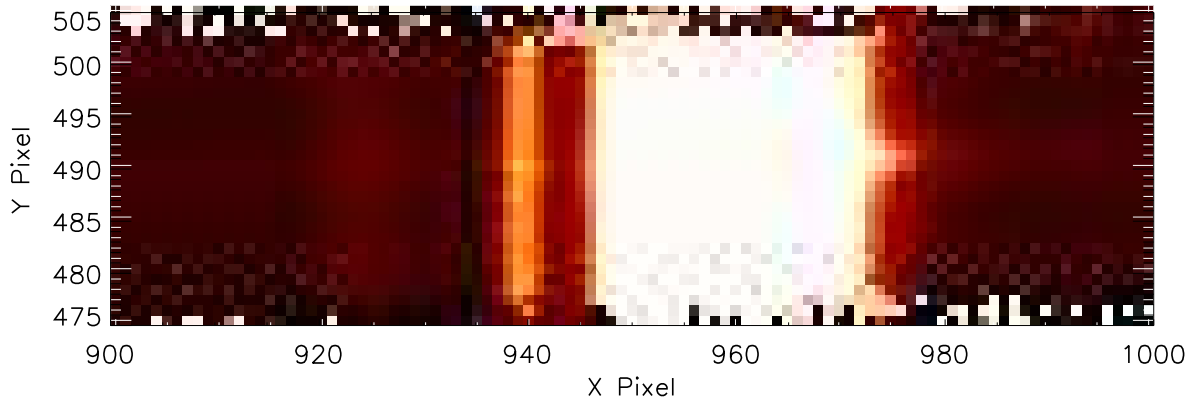


Fig. 2.— Flatfielded, cosmic-ray corrected raw image of the two spectra. Slit direction is vertical. The spectrum of 2MASS 0535–0546 is visible around pixel 490 on the Y-axis. Features extended on the vertical axis are due to deuterium and H $\alpha$  emission of the nebula, and to the night sky emission (Pixel 940). H $\alpha$  emission of 2MASS 0535–0546 appears on different sides of the nebula line in the two exposures.

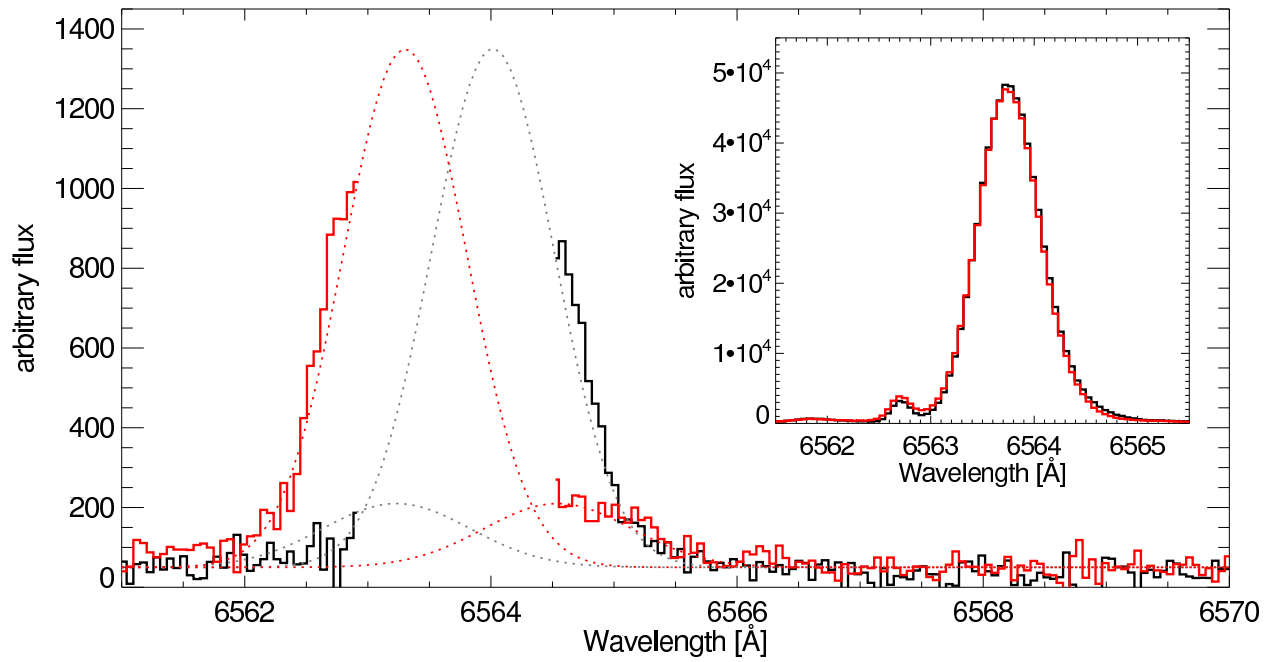


Fig. 3.— Region around the H $\alpha$  line. Solid lines are spectra #1 (black) and #2 (red) with nebula and sky emission removed. The inset shows the original data before the removal. We fit two Gaussians to each spectrum (see text). Individual components are plotted as dotted lines, different colors correspond to the different spectra.